Study of Temperature–Corrosion–Torsion Affecting Factors on the Shape of a Toroidal LPG Tank Using the Finite Element Method

Assoc. Prof. PhD. Eng. **Mihai ŢĂLU**[1], Assoc. Prof. PhD. Eng. **Ștefan ŢĂLU**[2,*]

[1] University of Craiova, Faculty of Mechanics, Department of Applied Mechanics and Civil Engineering, Calea București Street, no. 107, 200512 Craiova, Dolj county, Romania. E-mail: mihai_talu@yahoo.com

[2] Technical University of Cluj-Napoca, The Directorate of Research, Development and Innovation Management (DMCDI), Constantin Daicoviciu Street, no. 15, Cluj-Napoca, 400020, Cluj county, Romania. Corresponding author* e-mail: stefan_ta@yahoo.com

Abstract: *In this paper it is investigated the influence of the temperature–corrosion–torsion affecting factors on the shape of a three-dimensional (3-D) hexagonal toroid with regular hexagonal cross-section used in manufacturing of liquefied petroleum gas (LPG) storage tanks from the automotive industry. A design strategy was proposed to determine based on the finite element method, the change of the torsion angle, temperature and corrosion factors during operation. Numerical simulations were applied to compute the optimum form and sizing of the storage tank based on an objective optimization function to minimize the storage tank mass. The proposed method is demonstrated and numerical tested, demonstrating the potential of the suggested approach.*

Keywords: *3-D hexagonal toroidal LPG fuel tank, automotive industry, industrial engineering design, optimization methods*

1. Introduction

Nowadays, computer-aided design is recognized as a strategic resource in the field of the fuel tank industry [1-3] and a coherent approach regarding the advanced design tools [4-7] for the creation of new products with high performances was applied [8-10].
Diverse methods for manufacturing of LPG storage tanks have been introduced in many academic and industrial fields [11-14]. Most of them were made by approaches depended on the knowledge and experience of the experts concerning qualitative innovation based on 3-D design that offers a competitive advantage [14-17].
In the scientific literature there are presented various multicriteria analyses by evolutionary stages (design, execution and operation) [18-22] of the factors that influence LPG storage tanks from the automotive industry [23-26].
The dynamics of the storage tank markets requires superior engineering CAD designs [27-30], quality construction practices [31-33], and intelligent innovations for optimizing system performance and to meet the customers' requirements [33-36].
Modeling prototypes with computer-aided design (CAD) software [37-40] and advanced design modeling with a widely used interface standard [41-43] allow encouraging the rapid adoption of efficient technologies for LPG storage tanks including credible information, standards, and other management policies. Also, well-designed LPG storage tanks and control strategies can improve reliability, and reduce costs by using modern technologies [44-48].

2. Design methodology

2.1. Basic geometry of the parametric 3-D model

Let's consider the parametric 3-D model generated by revolving of a closed generating curve C_G (a hexagon with rounded corners) along a closed guiding curve C_D (a hexagon with rounded corners) as shown in figs. 1 and 2 [14].
The following parameters were applied as input parameters to the 3-D parametric model (figs. 1 and 2): a) a closed generating curve CG (a hexagon with a side value L = 175 mm, with rounded corners, radius R = 50 mm), and b) the guiding curve CD (a hexagon with a side value L = 430 mm, with rounded corners, radius R = 180 mm), and the thickness = 10 mm.

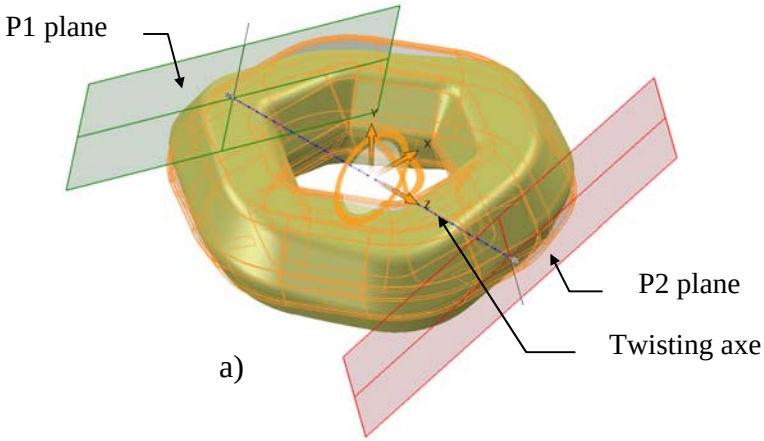

Fig. 1. The axonometric view of 3-D twisted model

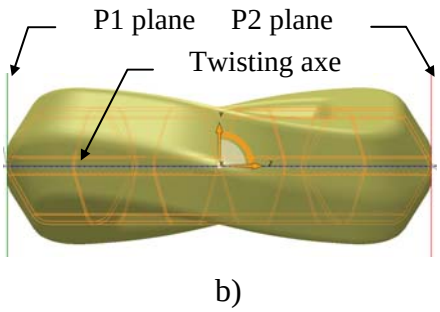

Fig. 2. The frontal view of 3-D twisted model

2.2. Numerical analysis of the parametric 3-D model

Based on the physical model, the modeling was done in the AutoCAD Autodesk 2020 software [49] and the numerical analysis was performed with SolidWorks 2020 software [50] with the Static, Thermal and Design Study modules. The design data used were:

- the tank material is AISI 4340 steel;
- the maximum hydraulic test pressure: p_{max} = 30 bar;
- the working temperature between the limits: T = -30 ^{0}C up to T = 60 ^{0}C;
- supporting surfaces located on the inferior side;
- the duration of the tank exploitation: n_a = 15 years;
- the corrosion rate of the material: v_c = 0.07 mm/year.

Numerical calculations were performed for: mesh standard type, solid mesh, curvature-based mesh with quality high, Jacobian in 16 points, element size 6 mm, number of nodes 47767, number of elements 23925.

The parameterized 3-D model used in calculus is a section of ½ (fig. 3) from the initial physical model and the corresponding surfaces to which the constraints and restrictions are applied are shown in fig. 4.

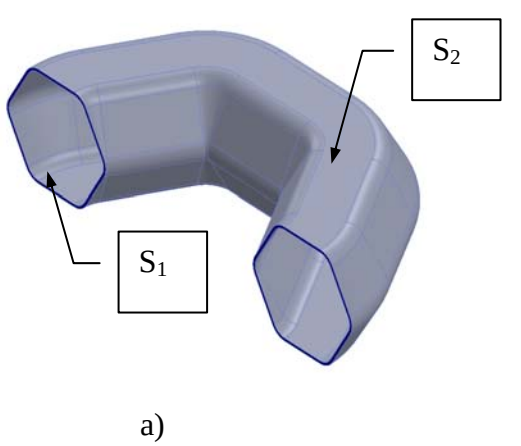

Fig. 3. The corresponding surfaces to which the constraints are applied for half section of the model

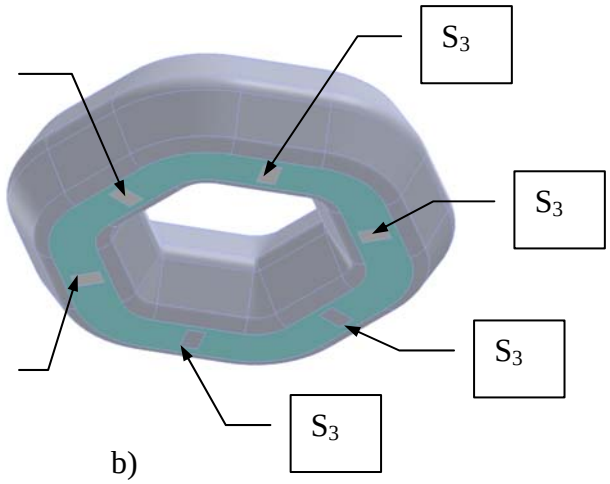

Fig. 4. The corresponding surfaces to which the constraints are applied for of the whole model

The design data used in this analysis for the tank lateral cover are:
- the maximum pressure p_{max} = 3 N/mm^2 on the inner surface S_1;
- the working temperature between the limits: T = -30 ^{0}C to T = 60 ^{0}C on the exterior surface S_2;
- the fixation of the tank on the six tank supports located at the inferior part of the tank.

The values of the state of stress Von Mises determined by the finite element method for n_a= 0 and 5 years are shown in table 1.

Table 1: The Von Mises resultant effort for n_a= 0 and 5 years

σ [MPa]	n_a= 0 years				n_a= 5 years			
	T [°C]				T [°C]			
ϕ [°]	-30°	0°	30°	60°	-30°	0°	30°	60°
0	604.130	533.813	441.46	487.942	609.754	513.007	455.0307	506.921
0.25	633.167	524.136	471.115	515.153	646.455	544.486	499.540	549.939
1	632.577	526.742	448.32	497.578	630.826	527.699	499.485	542.929
2	603.872	514.467	435.172	482.933	648.021	556.001	468.075	513.643
4	582.163	491.112	436.272	474.882	647.333	553.428	468.162	506.284
6	614.474	533.706	433.225	461.236	671.966	558.710	455.288	494.191
8	562.664	483.278	434.062	482.022	684.722	593.138	503.395	529.039
10	597.586	508.453	428.215	456.060	646.973	558.237	472.069	520.390

The graphs corresponding to the Von Mises resultant efforts taking into account the results from table 1 are graphically shown in figs. 7, 8, 13 and 14, respectively.
The most important cases of the maximum values of the Von Mises effort taking into account the results from table 2 are graphically shown in figs. 5, 6, 9, 10, 11, 12, 15 and 16, respectively.

Table 2: The maximum values of the Von Mises resultant effort

Case no.	n_a [years]	ϕ [°]	T [°C]	σ [MPa]
1	0	0.25	-30	633.167
2	5	8	-30	684.722
3	10	0.25	-30	671.250
4	15	8	-30	726.248

a) Case no.1

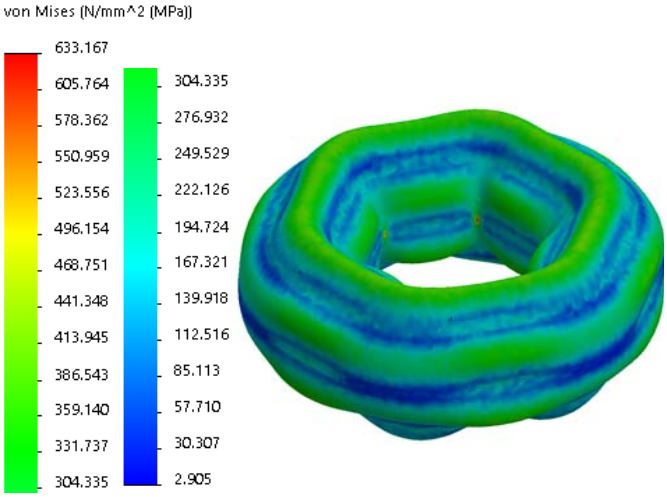

Fig. 5. The graphs of Von Mises stress distribution for n_a = 0 years

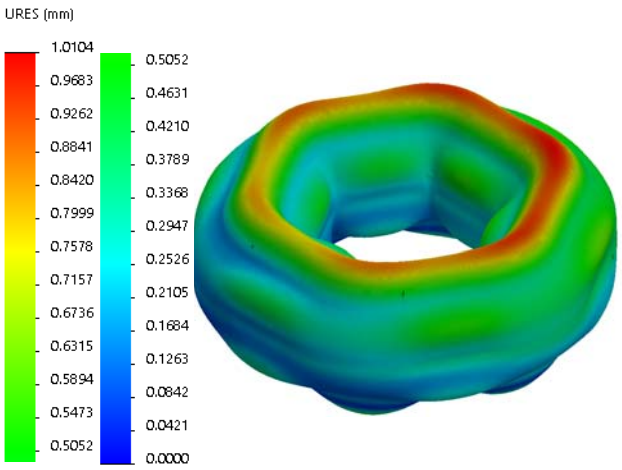

Fig. 6. The graphs of linear deformation distribution for n_a = 0 years

The graphs of 3-D surfaces corresponding to the Von Mises effort σ = f(T, ϕ) for 0 and 5 years are graphically shown in figs. 7 and 8.

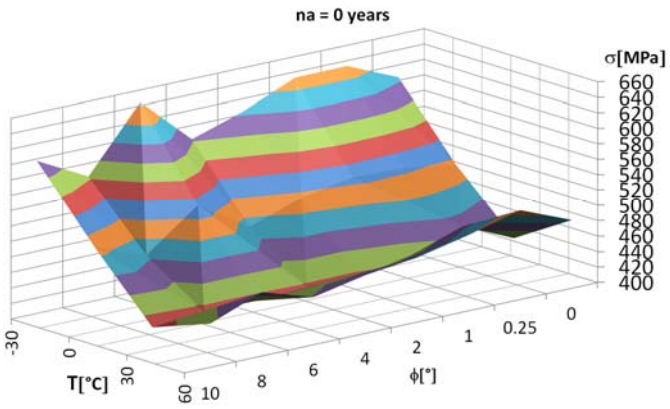

Fig. 7. The graphs of $\sigma = f(T, \phi)$ for n_a = 0 years

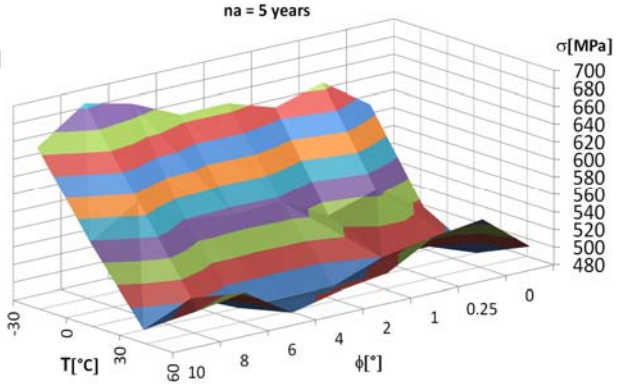

Fig. 8. The graphs of $\sigma = f(T, \phi)$ for n_a = 5 years

b) Case no. 2

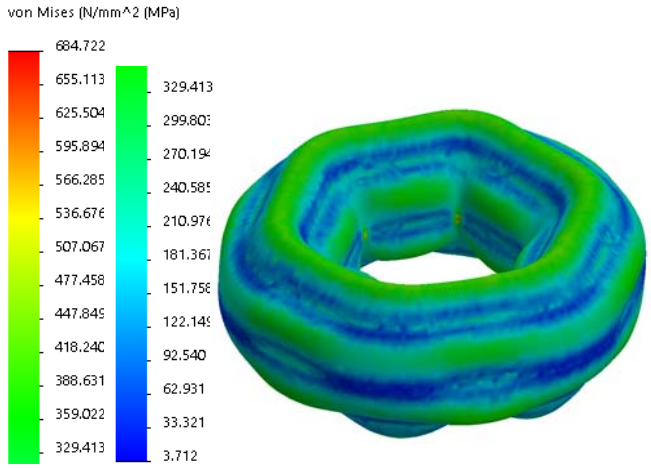

Fig. 9. The graphs of Von Mises stress distribution for n_a = 5 years

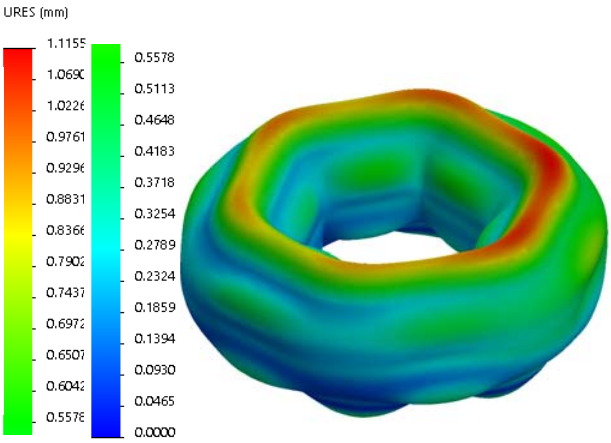

Fig. 10. The graphs of linear deformation distribution for n_a = 5 years

The values of the state of stress Von Mises determined by the finite element method for n_a= 10 and 15 years are shown in table 3.

Table 3: The Von Mises resultant effort for n_a= 10 and 15 years

σ [MPa]	n_a= 10 years				n_a= 15 years			
	T [°C]				T [°C]			
ϕ [°]	-30°	0°	30°	60°	-30°	0°	30°	60°
0	631.859	536.113	500.095	544.749	664.749	580.277	539.257	593.356
0.25	671.825	580.275	513.908	559.111	720.992	642.609	563.393	609.903
1	656.152	558.748	523.648	572.092	690.050	582.294	575.271	617.743
2	640.331	548.530	499.530	544.232	656.473	556.017	565.732	612.368
4	665.269	566.368	511.877	560.938	697.559	602.885	560.280	614.595
6	618.443	539.903	498.637	551.038	675.154	587.652	540.631	594.554
8	642.592	555.988	519.963	572.506	726.248	633.716	542.715	587.319
10	637.352	547.513	501.518	553.876	677.954	585.842	565.737	613.592

c) Case no. 3

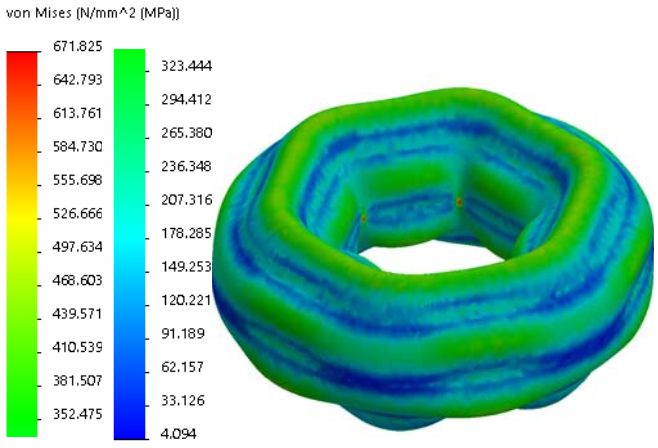

Fig. 11. The graphs of Von Mises stress distribution for n_a = 10 years

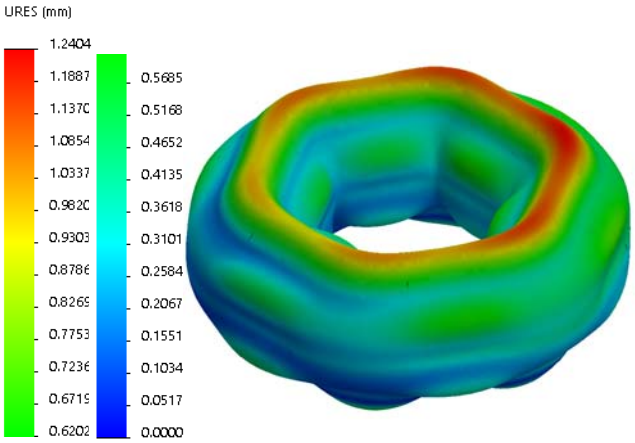

Fig. 12. The graphs of linear deformation distribution for n_a = 10 years

The graphs of 3-D surfaces corresponding to the Von Mises effort $\sigma = f(T, \phi)$ for 10 and 15 years are graphically shown in figs. 13 and 14.

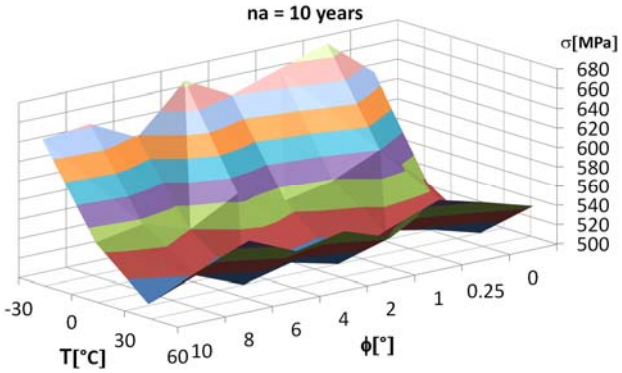

Fig. 13. The graphs of $\sigma = f(T, \phi)$ for n_a =10 years

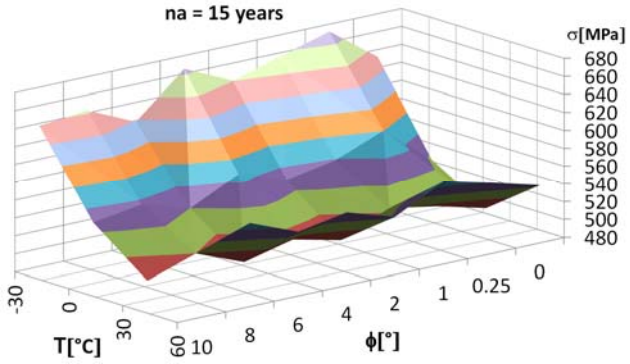

Fig. 14. The graphs of $\sigma = f(T, \phi)$ for n_a = 15 years

d) Case no. 4

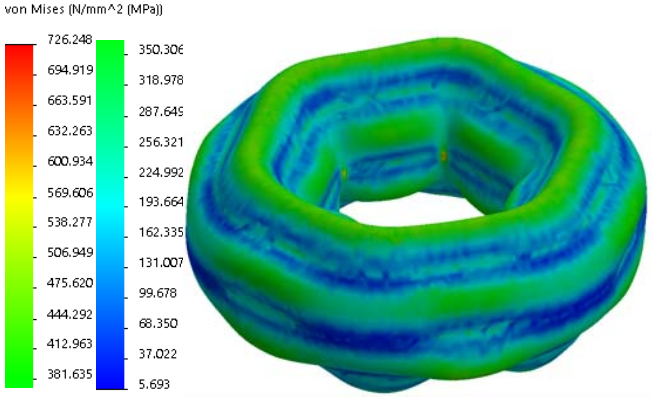

Fig. 15. The graphs of Von Mises stress distribution for n_a = 15 years

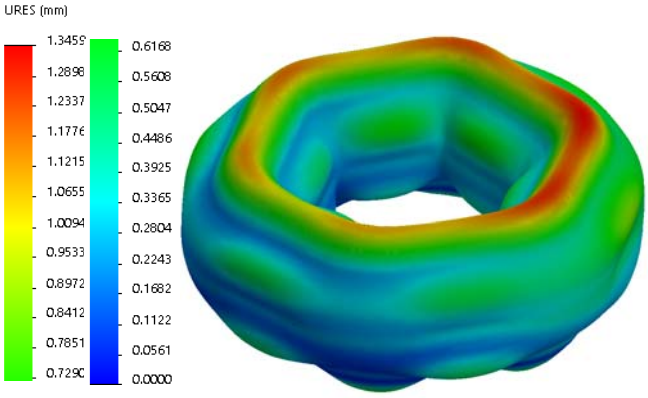

Fig. 16. The graphs of linear deformation distribution for n_a = 15 years

The percentage variation of Von Mises resultant effort in relation to the initial effort status (tables 4 and 5) and the corresponding graphs are given in figs. 17, 18 and 19.

Table 4: The percentage variation of Von Misess resultant effort for 5 and 10 years

	$\Delta\sigma$ [%] for n_a= 5 years				$\Delta\sigma$ [%] for n_a= 10 years			
	T [°C]				T [°C]			
ϕ [°]	-30°	0°	30°	60°	-30°	0°	30°	60°
0	0.93	3.74	3.07	3.89	4.59	4.34	13.28	11.64
0.25	2.10	3.88	6.03	6.75	6.11	10.71	9.08	8.53
1	0.99	0.18	11.41	9.11	3.73	6.08	16.80	14.98
2	7.31	8.07	7.56	6.36	6.04	6.62	14.79	12.69
4	11.19	12.69	7.31	6.61	14.28	15.32	17.33	18.12
6	9.36	4.68	5.09	7.14	0.65	1.16	15.10	19.47
8	21.69	22.73	15.97	9.75	14.21	15.05	19.79	18.77
10	8.26	9.79	10.24	14.11	6.65	7.68	17.12	21.45

Table 5: The percentage variation of Von Misess resultant effort for 15 years

	$\Delta\sigma$ [%] for n_a = 15 years			
	T [°C]			
	-30°	0°	30°	60°
ϕ [°]	10.03	12.94	22.15	21.60
0	13.87	22.60	19.59	18.39
0.25	9.09	10.55	28.32	24.15
1	8.71	8.08	30.00	26.80
2	19.82	22.76	28.42	29.42
4	9.88	10.11	24.79	28.90
6	29.07	31.13	25.03	21.84
8	13.45	15.22	32.12	34.54
10	10.03	12.94	22.15	21.60

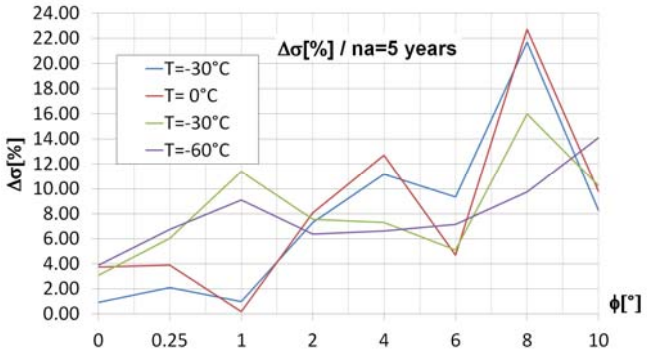

Fig. 17. The graphs of $\Delta\sigma$ for n_a = 5 years

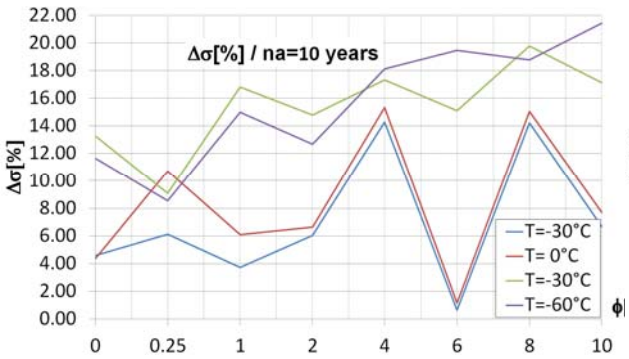

Fig. 18. The graphs of $\Delta\sigma$ for n_a = 10 years

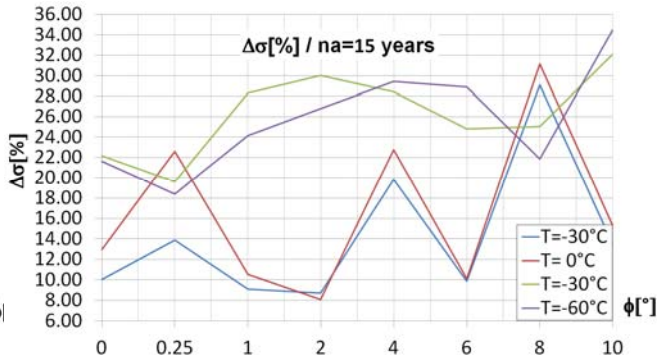

Fig. 19. The graphs of $\Delta\sigma$ for n_a = 15 years

The most important cases of the maximum values of the resultant linear deformation taking into account the results from table 6 are graphically shown in figs. 20, 21, 24, 25, 26, 27, 30 and 31, respectively.
The graphs corresponding to the resultant linear deformation *u* taking into account the results from table 6 are graphically shown in figs. 22, 23, 28 and 29, respectively.
The values of the resultant linear deformation *u* determined by the finite element method for 0 and 5 years are shown in table 6.

Table 6: The resultant linear deformation for n_a= 0 and 5 years

u [mm]	n_a= 0 years				n_a= 5 years			
	T [°C]				T [°C]			
ϕ [°]	-30°	0°	30°	60°	-30°	0°	30°	60°
0	1.0170	0.9791	0.9434	0.9117	1.11340	1.0743	1.0369	1.0043
0.25	1.01801	0.97955	0.94958	0.9262	1.12945	1.09517	1.06171	1.03081
1	0.99508	0.96169	0.93050	0.90255	1.08137	1.04716	1.01438	0.98266
2	0.97581	0.94611	0.91779	0.89117	1.06893	1.03666	1.00558	0.97721
4	0.99898	0.96650	0.93499	0.90532	1.08680	1.05429	1.02450	0.99571
6	1.02196	0.98997	0.96063	0.93327	1.12669	1.09292	1.06090	1.02826
8	1.01696	0.98608	0.95619	0.92772	1.11552	1.08383	1.05303	1.02509
10	1.03229	1.00131	0.97133	0.94276	1.13948	1.08960	1.07938	1.05072

Table 7: The maximum values of the resultant linear deformation

Case no.	n_a [years]	ϕ [°]	T [°C]	u [mm]
5	0	0	-30	1.01700
6	5	10	-30	1.13948
7	10	10	-30	1.24760
8	15	10	-30	1.38699

e) Case no. 5

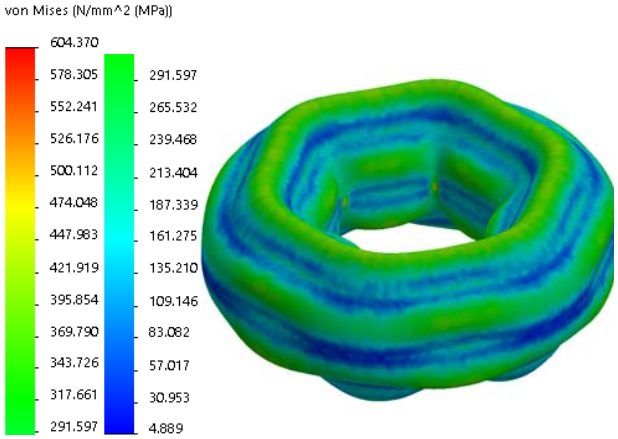

Fig. 20. The graphs of Von Mises stress distribution for n_a = 0 years

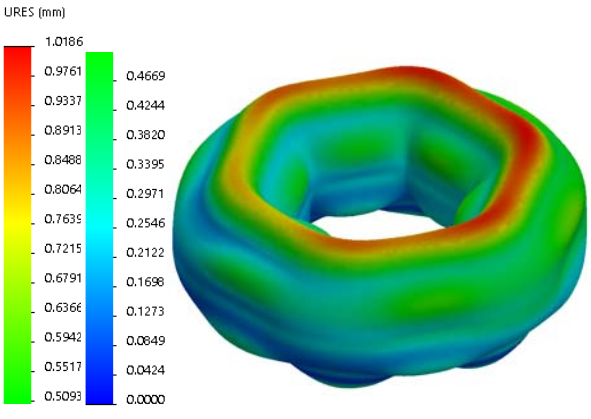

Fig. 21. The graphs of linear deformation distribution for n_a = 0 years

The graphs of 3-D surfaces corresponding to the resultant linear deformation for 0 and 5 years are graphically shown in figs. 22 and 23.

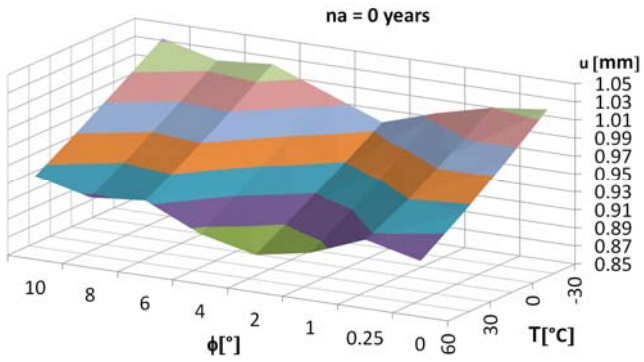

Fig. 22. The graphs of u = f(T, ϕ) for n_a = 0 years

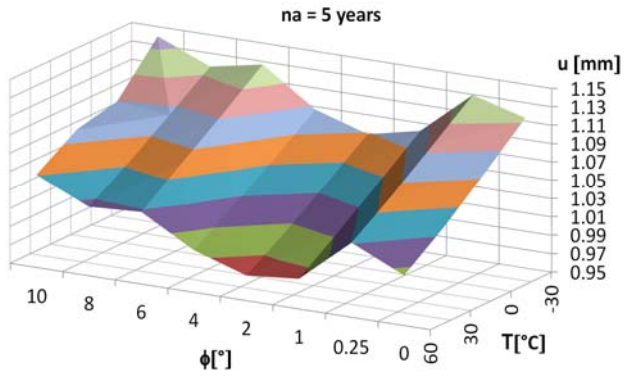

Fig. 23. The graphs of u = f(T, ϕ) for n_a = 5 years

f) Case no. 6

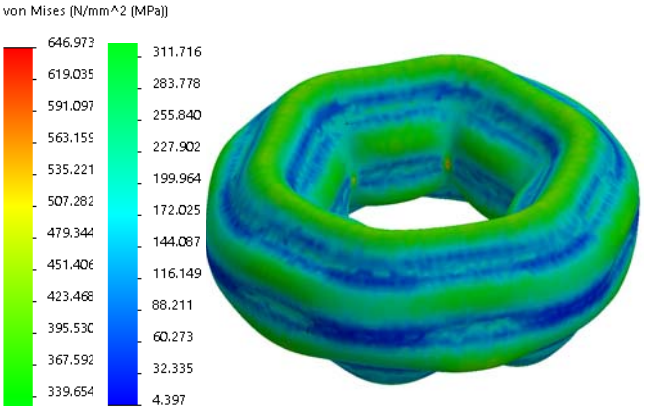

Fig. 24. The graphs of Von Mises stress distribution for n_a = 5 years

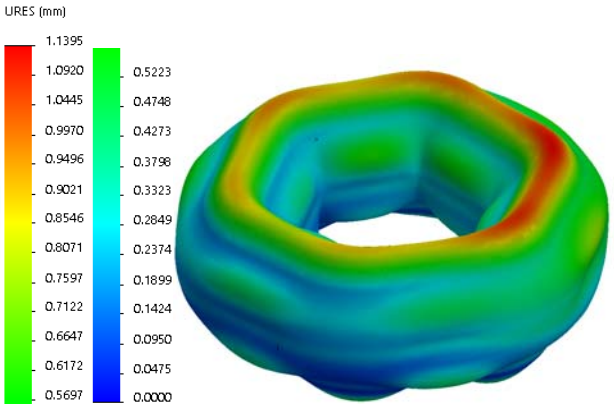

Fig. 25. The graphs of linear deformation distribution for n_a = 5 years

The values of the resultant linear deformation u determined by the finite element method for 10 and 15 years are shown in table 8.

Table 8: The resultant linear deformation for n_a= 10 and 15 years

u [mm]	n_a= 10 years				n_a= 15 years			
	T [°C]				T [°C]			
ϕ [°]	-30°	0°	30°	60°	-30°	0°	30°	60°
0	1.2272	1.1873	1.149	1.115	1.350	1.309	1.269	1.234
0.25	1.24041	1.20394	1.16825	1.13343	1.35984	1.32258	1.28607	1.25023
1	1.19863	1.16424	1.13162	1.10273	1.31771	1.28140	1.24605	1.22414
2	1.1848	1.15216	1.12050	1.09030	1.30078	1.26603	1.23383	1.20218
4	1.19040	1.15660	1.12632	1.09682	1.33552	1.27958	1.24871	1.21853
6	1.23481	1.20082	1.16787	1.13583	1.35532	1.32053	1.28648	1.25324
8	1.23110	1.19687	1.16377	1.13202	1.34585	1.31439	1.28365	1.2537
10	1.24760	1.21373	1.18070	1.14858	1.38699	1.35259	1.31891	1.28601

g) Case no. 7

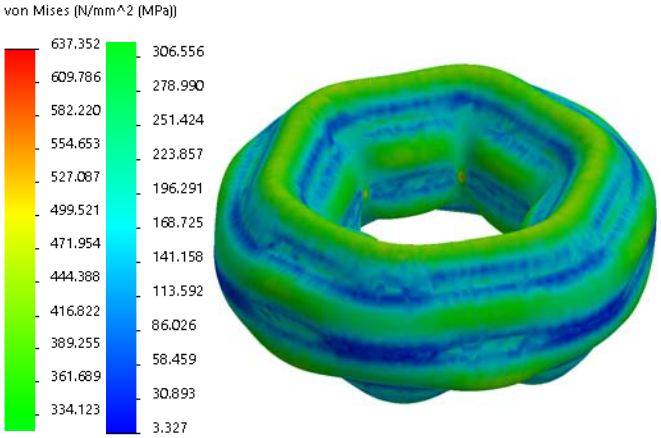

Fig. 26. The graphs of Von Mises stress distribution for n_a = 10 years

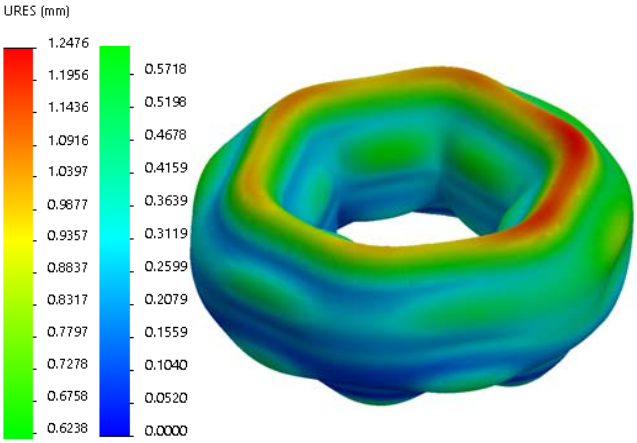

Fig. 27. The graphs of linear deformation distribution for n_a = 10 years

The graphs of 3-D surfaces corresponding to the resultant linear deformation for 10 and 15 years are graphically shown in figs. 28 and 29.

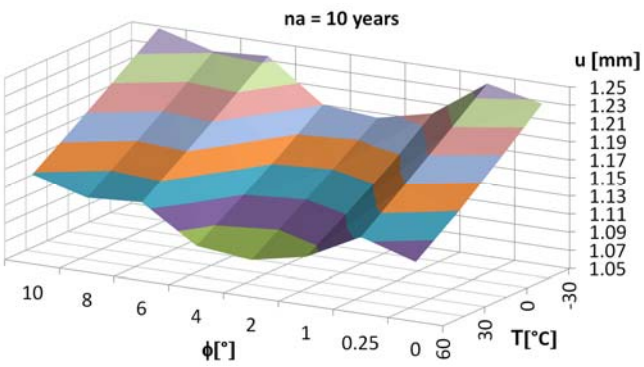

Fig. 28. The graphs of u = f(T, ϕ) for n_a = 10 years

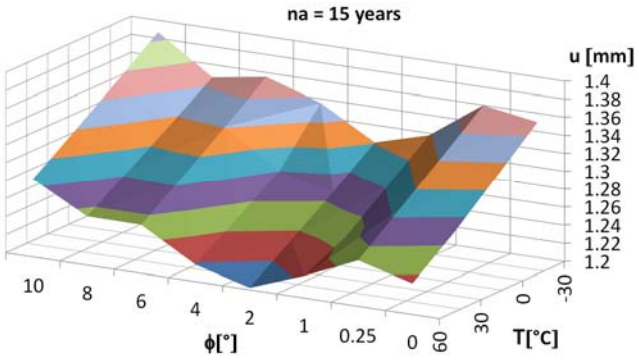

Fig. 29. The graphs of u = f(T, ϕ) for n_a = 15 years

h) Case no. 8

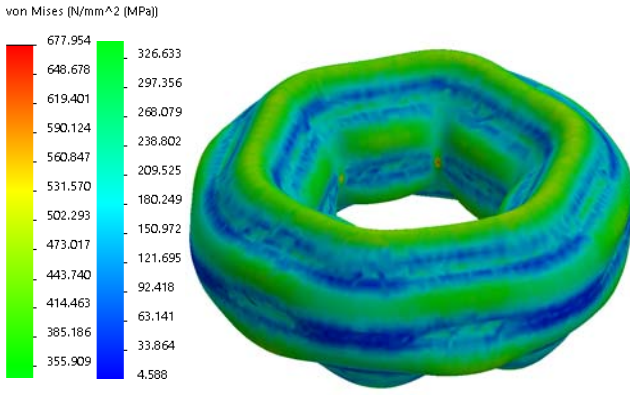

Fig. 30. The graphs of Von Mises stress distribution for n_a = 15 years

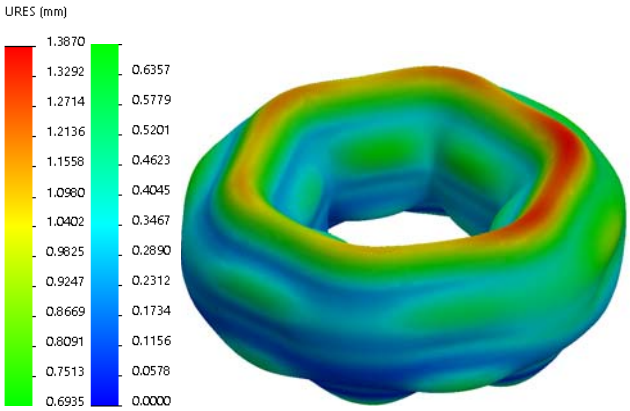

Fig. 31. The graphs of linear deformation distribution for n_a = 15 years

The percentage variation of resultant linear deformation in relation to the initial value (tables 9 and 10) and the corresponding graphs are given in figs. 32, 33 and 34.

Table 9: The percentage variation of resultant linear deformation for 5 and 10 years

	Δu [%] for n_a= 5 years				Δu [%] for n_a= 10 years			
	T [°C]				T [°C]			
ϕ [°]	-30°	0°	30°	60°	-30°	0°	30°	60°
0	9.48	9.72	9.91	10.16	20.67	21.26	21.79	22.30
0.25	11.83	11.80	11.81	11.29	22.81	22.91	23.03	22.37
1	8.67	8.89	9.01	8.88	20.46	21.06	21.61	22.18
2	9.54	9.57	9.57	9.65	21.42	21.78	22.09	22.34
4	8.79	9.08	9.57	9.98	19.16	19.67	20.46	21.15
6	10.25	10.40	10.44	10.18	20.83	21.30	21.57	21.70
8	9.69	9.91	10.13	10.50	21.06	21.38	21.71	22.02
10	10.38	8.82	11.12	11.45	20.86	21.21	21.55	21.83

Table 10: The percentage variation of resultant linear deformation for 15 years

	Δu [%] for n_a= 15 years			
	T[°C]			
ϕ [°]	-30°	0°	30°	60°
0	32.74	33.69	34.51	35.35
0.25	34.64	35.02	35.44	34.98
1	32.42	33.24	33.91	35.63
2	33.30	33.81	34.43	34.90
4	33.69	32.39	33.55	34.60
6	32.62	33.39	33.92	34.28
8	32.34	33.29	34.25	35.14
10	34.36	35.08	35.78	36.41

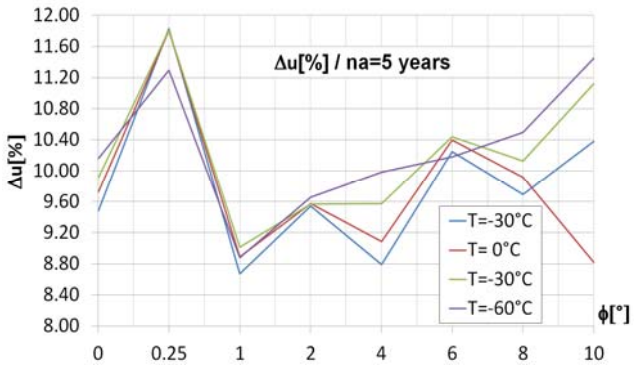

Fig. 32. The graphs of Δu for n_a = 5 years

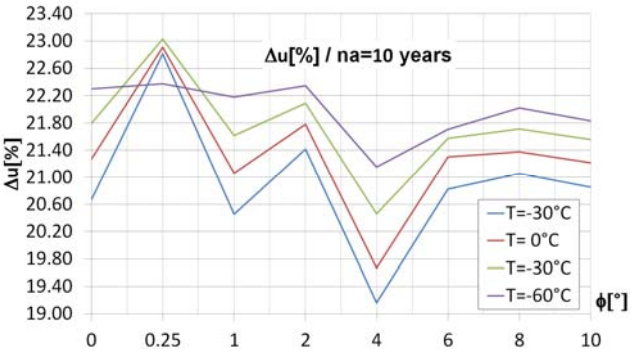

Fig. 33. The graphs of Δu for n_a = 10 years

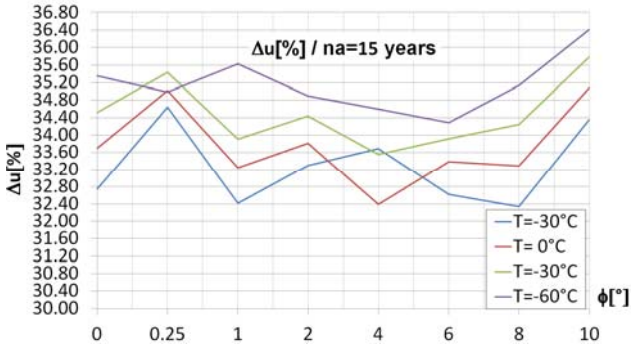

Fig. 34. The graphs of Δu for n_a = 15 years

3. Conclusions

Following the numerical analyses and the resulting graphs it has been found that:
- with the increase of the torsion angle ϕ, the state of effort increases and reaches maximum values with the decreasing of the temperature, reaching a minimum value for T = -30 ^{0}C;
- the state of efforts are amplified with the increase of corrosion, by decreasing the thickness of the wall of the tank coverings;
- in the last year of exploitation (n_a= 15 years), the maximum value of the Von Mises stress occurs at T = - 30 ^{0}C, ϕ = 8 [°], and σ = 726.25 MPa > σ_a = 710 MPa;
- the percentage variation of Von Mises resultant effort in report with n_a= 0 years, indicated an increasing of Δσ [%] > 34.54 [%] for T = 60 ^{0}C. Also, the resultant linear deformation *u* has a maximum value for ϕ = 10 [°] and T = -30 ^{0}C. The percentage variation of resultant linear deformation Δu [%] has a maximum value for maximum values of ϕ and T.
- the results shows that the angular torsion overlaps over the disadvantageous effects of corrosion and temperature variation leading to higher increases of stress and deformation states.

References

[1] Ghiţă, C. Mirela, Anton C. Micu, Mihai Ţălu and Ştefan Ţălu. "Shape optimization of a thoroidal methane gas tank for automotive industry." *Annals of Faculty of Engineering Hunedoara - International Journal of Engineering, Hunedoara, Romania*, Tome X, Fascicule 3 (2012): 295-297.
[2] Ghiţă, C. Mirela, Anton C. Micu, Mihai Ţălu and Ştefan Ţălu. "Shape optimization of vehicle's methane gas tank." *Annals of Faculty of Engineering Hunedoara - International Journal of Engineering, Hunedoara, Romania*, Tome X, Fascicule 3 (2012): 259-266.
[3] Ghiţă, C. Mirela, Anton C. Micu, Mihai Ţălu, Ştefan Ţălu and Ema I. Adam. "Computer-Aided Design of a classical cylinder gas tank for the automotive industry." *Annals of Faculty of Engineering Hunedoara - International Journal of Engineering, Hunedoara*, *Romania*, Tome XI, Fascicule 4 (2013): 59-64.

[4] Ghiţă, C. Mirela, Anton C. Micu, Mihai Ţălu and Ştefan Ţălu. "3D modelling of a shrink fitted concave ended cylindrical tank for automotive industry." *Acta Technica Corviniensis – Bulletin of Engineering, Hunedoara, Romania*, Tome VI, Fascicule 4 (2013): 87-92.
[5] Ghiţă, C. Mirela, Anton C. Micu, Mihai Ţălu and Ştefan Ţălu. "3D modelling of a gas tank with reversed end up covers for automotive industry.", *Annals of Faculty of Engineering Hunedoara - International Journal of Engineering, Hunedoara*, *Romania*, Tome XI, Fascicule 3 (2013): 195-200.
[6] Ghiţă, C. Mirela, Ştefan C. Ghiţă, Ştefan Ţălu and Simona Rotaru, "Optimal design of cylindrical rings used for the shrinkage of vehicle tanks for compressed natural gas." *Annals of Faculty of Engineering Hunedoara - International Journal of Engineering, Hunedoara*, Tome XII, Fascicule 3 (2014): 243-250.
[7] Bică, Marin, Mihai Ţălu and Ştefan Ţălu. "Optimal shapes of the cylindrical pressurized fuel tanks." *Magazine of Hydraulics, Pneumatics, Tribology, Ecology, Sensorics, Mechatronics (HIDRAULICA)*, no. 4 (December 2017): 6-17.
[8] Vintilă, Daniela, Mihai Ţălu and Ştefan Ţălu. "The CAD analyses of a torospheric head cover of a pressurized cylindrical fuel tank after the crash test." *Magazine of Hydraulics, Pneumatics, Tribology, Ecology, Sensorics, Mechatronics (HIDRAULICA)*, no. 4 (December 2017): 57-66.
[9] Ţălu, Ştefan and Mihai Ţălu. "The influence of deviation from circularity on the stress of a pressurized fuel cylindrical tank." *Magazine of Hydraulics, Pneumatics, Tribology, Ecology, Sensorics, Mechatronics (HIDRAULICA)*, no. 4 (December 2017): 34-45.
[10] Ţălu, Mihai. "The influence of the corrosion and temperature on the Von Mises stress in the lateral cover of a pressurized fuel tank." *Magazine of Hydraulics, Pneumatics, Tribology, Ecology, Sensorics, Mechatronics (HIDRAULICA)*, no. 4 (December 2017): 89-97.
[11] Ţălu, Mihai and Ştefan Ţălu. "Analysis of temperature resistance of pressurized cylindrical fuel tanks." *Magazine of Hydraulics, Pneumatics, Tribology, Ecology, Sensorics, Mechatronics (HIDRAULICA)*, no. 1 (March 2018): 6-15.
[12] Ţălu, Mihai and Ştefan Ţălu. "Design and optimization of pressurized toroidal LPG fuel tanks with variable section." *Magazine of Hydraulics, Pneumatics, Tribology, Ecology, Sensorics, Mechatronics (HIDRAULICA)*, no. 1 (March 2018): 32-41.
[13] Ţălu, Ştefan and Mihai Ţălu. "Algorithm for optimal design of pressurized toroidal LPG fuel tanks with constant section described by imposed algebraic plane curves." *Magazine of Hydraulics, Pneumatics, Tribology, Ecology, Sensorics, Mechatronics (HIDRAULICA)*, no. 2 (June 2018): 14-21.
[14] Ţălu, Mihai and Ştefan Ţălu. "The optimal CAD design of a 3D hexagonal toroid with regular hexagonal cross-section used in manufacturing of LPG storage tanks." *Magazine of Hydraulics, Pneumatics, Tribology, Ecology, Sensorics, Mechatronics (HIDRAULICA)*, no. 2 (June 2018): 49-56.
[15] Ţălu, Mihai and Ştefan Ţălu. "The influence of corrosion and temperature variation on the minimum safety factor of a 3D hexagonal toroid with regular hexagonal cross-section used in manufacturing of LPG storage tanks." *Magazine of Hydraulics, Pneumatics, Tribology, Ecology, Sensorics, Mechatronics (HIDRAULICA)*, no. 3 (August 2018): 16-25.
[16] Ţălu, Ştefan and Mihai Ţălu. "The influence of corrosion and pressure variation on the minimum safety factor of a 3D hexagonal toroid with regular hexagonal cross-section used in manufacturing of LPG storage tanks." *Magazine of Hydraulics, Pneumatics, Tribology, Ecology, Sensorics, Mechatronics (HIDRAULICA)*, no. 3 (August 2018): 39-45.
[17] Ţălu, Mihai and Ştefan Ţălu. "The influence of corrosion and temperature variation on a CNG storage tank with a combined form consisting of a torus and a sphere." *Magazine of Hydraulics, Pneumatics, Tribology, Ecology, Sensorics, Mechatronics (HIDRAULICA)*, no. 4 (December 2019): 93-104.
[18] Ţălu, Mihai and Ştefan Ţălu. "Optimal design of a CNG storage tank with a combined form consisting of a torus and a sphere." *Magazine of Hydraulics, Pneumatics, Tribology, Ecology, Sensorics, Mechatronics (HIDRAULICA)*, no. 4 (December 2019): 73-82.
[19] Ţălu, Ştefan and Mihai Ţălu. "Numerical analysis of the influence of uniaxial compression loads on the shape of a toroidal LPG tank." *Magazine of Hydraulics, Pneumatics, Tribology, Ecology, Sensorics, Mechatronics (HIDRAULICA)*, no. 1 (March 2020): 47-58.
[20] Ţălu, Mihai and Ştefan Ţălu. "Stress and deformation analysis under bending and torsional loads of a toroidal LPG tank based on the finite element analysis." *Magazine of Hydraulics, Pneumatics, Tribology, Ecology, Sensorics, Mechatronics (HIDRAULICA)*, no. 1 (March 2020): 88-101.
[21] Ţălu, Mihai and Ştefan Ţălu. "3D geometrical solutions for toroidal LPG fuel tanks used in automotive industry." *Advances in Intelligent Systems Research,* vol. 151 (2018): 189-193. DOI: 10.2991/cmsa-18.2018.44.
[22] Ţălu, Ştefan and Mihai Ţălu. "Constructive CAD variants of toroidal LPG fuel tanks used in automotive Industry." *Advances in Intelligent Systems Research,* vol. 159 (2018): 27-30. DOI: 10.2991/mmsa-18.2018.7.

[23] Ţălu, Ştefan and Mihai Ţălu. "The Influence of corrosion on the vibration modes of a pressurized fuel tank used in automotive industry." *DEStech Transactions on Materials Science and Engineering,* (2018): 1-6. DOI: 10.12783/dtmse/icmsa2018/20560.
[24] Ţălu, Mihai and Ştefan Ţălu. "Optimal engineering design of a pressurized paralepipedic fuel tank." *Annals of Faculty of Engineering Hunedoara - International Journal of Engineering, Hunedoara, Romania*, Tome XVI, Fascicule 2 (2018): 193-200.
[25] Malviya, Rupesh Kumar and Muhamed Rushaid. "Consequence analysis of LPG storage tank." Materials today, vol. 5, issue 2 (2018): 4359-4367. DOI: 10.1016/j.matpr.2017.12.003.
[26] Ejeh, Chukwugozie Jekwu, Akhabue Gbemisola Precious and Isaac Agyeibi. "Effect of transient temperature on 304 stainless steel LPG tank structure using numerical simulation approach." *SN Applied Sciences,* no. 1, (2019): article number: 1690. DOI: 10.1007/s42452-019-1760-1.
[27] Ţălu, Ştefan and Mihai Ţălu. "CAD generating of 3D supershapes in different coordinate systems." *Annals of Faculty of Engineering Hunedoara - International Journal of Engineering, Hunedoara, Romania*, Tome VIII, Fascicule 3 (2010): 215-219.
[28] Ţălu, Ştefan and Mihai Ţălu. "A CAD study on generating of 2D supershapes in different coordinate systems." *Annals of Faculty of Engineering Hunedoara - International Journal of Engineering, Hunedoara, Romania*, Tome VIII, Fascicule 3 (2010): 201-203.
[29] Niţulescu, Theodor and Ştefan Ţălu. *Aplicaţii ale geometriei descriptive şi graficii asistate de calculator în desenul industrial. (Applications of descriptive geometry and computer aided design in engineering graphics).* Cluj-Napoca, Risoprint Publishing house, 2001.
[30] Bîrleanu, Corina and Ştefan Ţălu. *Organe de maşini. Proiectare şi reprezentare grafică asistată de calculator. (Machine elements. Designing and computer assisted graphical representations).* Cluj-Napoca, Victor Melenti Publishing house, 2001.
[31] Ţălu, Ştefan and Mihai Ţălu. *AutoCAD 2006. Proiectare tridimensională. (AutoCAD 2006. Three-dimensional designing)*. Cluj-Napoca, MEGA Publishing house, 2007.
[32] Ţălu, Ştefan. *Geometrie descriptivă. (Descriptive geometry)*, Cluj-Napoca, Risoprint Publishing house, 2010.
[33] Ţălu, Ştefan. *AutoCAD 2017*. Cluj-Napoca, Napoca Star Publishing house, 2017.
[34] Ţălu, Ştefan. *Micro and nanoscale characterization of three dimensional surfaces. Basics and applications*. Napoca Star Publishing House, Cluj-Napoca, Romania, 2015.
[35] Ţălu, Ştefan and Cristina Racocea. *Reprezentări axonometrice cu aplicaţii în tehnică. (Axonometric representations with applications in technique).* Cluj-Napoca, MEGA Publishing house, 2007.
[36] Racocea, Cristina and Ştefan Ţălu. *Reprezentarea formelor geometrice tehnice în axonometrie. (The axonometric representation of technical geometric shapes).* Cluj-Napoca, Napoca Star Publishing house, 2011.
[37] Ţălu, Mihai. *Calculul pierderilor de presiune distribuite în conducte hidraulice. (Calculation of distributed pressure loss in hydraulic pipelines).* Craiova, Universitaria Publishing house, 2016.
[38] Ţălu, Mihai. *Mecanica fluidelor. Curgeri laminare monodimensionale. (Fluid mechanics. The monodimensional laminar flow).* Craiova, Universitaria Publishing house, 2016.
[39] Ţălu, Mihai. *Pierderi de presiune hidraulică în conducte tehnice cu secţiune inelară. Calcul numeric şi analiză C.F.D. (Hydraulic pressure loss in technical piping with annular section. Numerical calculation and C.F.D.)*, Craiova, Universitaria Publishing house, 2016.
[40] Nedelcu, Dorian. *Proiectare şi simulare numerică cu SolidWorks*. *(Digital Prototyping and Numerical Simulation with SolidWorks)*. Timişoara, Eurostampa Publishing house, 2011.
[41] Florescu-Gligore, Adrian, Ştefan Ţălu and Dan Noveanu. *Reprezentarea şi vizualizarea formelor geometrice în desenul industrial. (Representation and visualization of geometric shapes in industrial drawing).* Cluj-Napoca, U. T. Pres Publishing house, 2006.
[42] Florescu-Gligore, Adrian, Magdalena Orban and Ştefan Ţălu. *Cotarea în proiectarea constructivă şi tehnologică. (Dimensioning in technological and constructive engineering graphics).* Cluj-Napoca, Lithography of The Technical University of Cluj-Napoca, 1998.
[43] Ţălu, Ştefan. *Limbajul de programare AutoLISP. Teorie şi aplicaţii. (AutoLISP programming language. Theory and applications)*. Cluj-Napoca, Risoprint Publishing house, 2001.
[44] Ţălu, Ştefan. *Grafică tehnică asistată de calculator. (Computer assisted technical graphics)*. Cluj-Napoca, Victor Melenti Publishing house, 2001.
[45] Ţălu, Ştefan. *Reprezentări grafice asistate de calculator. (Computer assisted graphical representations).* Cluj-Napoca, Osama Publishing house, 2001.
[46] Ţălu, Ştefan. *Tehnologia de rulare a filetelor. (Thread rolling technology).* Cluj-Napoca, Napoca Star Publishing house, 2019.
[47] *** Certification tests of LPG and CNG. Accessed March 3, 2020. http://vzlutest.cz/en/certification-tests-of-lpg-and-cng-c3.html.
[48] *** TANK software (https://cas.hexagonppm.com/solutions/tank)
[49] *** Autodesk AutoCAD 2020 software.
[50] *** SolidWorks 2020 software.